Available online at www.sciencedirect.com
SCIENCE DIRECT®
Physica E 21 (2004) 241–246
PHYSICA E
www.elsevier.com/locate/physe

Vibrational spectroscopy of InAs and AlAs quantum dot structures

A.G. Milekhin[a,*], A.I. Toropov[a], A.K. Bakarov[a], M.Yu. Ladanov[a], G. Zanelatto[b], J.C. Galzerani[b], S. Schulze[c], D.R.T. Zahn[c]

[a] *Institute of Semiconductor Physics, Lavrentjev av.13, Novosibirsk 630090, Russia*
[b] *Departamento de Fisica, Universidade Federal de Sao Carlos, C.P.676, Sao Carlos, SP, Brazil*
[c] *Institut für Physik, Technische Universität Chemnitz, Chemnitz D-09107, Germany*

Abstract

In this paper we present an experimental comparative study of InAs/AlAs periodical structures with InAs and AlAs quantum dots (QDs) by means of infrared and Raman spectroscopies. The first observation of optical phonons localized in InAs and AlAs QDs using infrared spectroscopy is demonstrated. Confined optical phonon frequencies of the QDs measured by means of Raman scattering are compared with those deduced from the analysis of infrared spectra performed in the framework of the dielectric function approximation.

PACS: 78.30.Fs; 78.67.Hc

Keywords: Infrared spectroscopy; Raman spectroscopy; Phonons; Quantum dots; Confinement

1. Introduction

Vibrational properties of semiconductor III_aV_b/III_cV_b periodical structures with reduced dimensionality (multi-quantum well structures, superlattices) have been the subject of a large number of experimental and theoretical investigations [1–6] and fairly well understood. Systematic studies of lattice vibrations in such layered strained and strain-free periodical structures with layer thickness of even few monolayers have been performed by Raman scattering, where longitudinal optical (LO) phonons are active in the usual backscattering geometry from (0 0 1) crystal planes. Little information is available about transverse optical (TO) phonons since Raman scattering by TO phonons requires significant experimental efforts. Infrared reflectivity is sensitive to both TO and LO confined phonons in planar ultra-thin layered structures appearing at poles and zeros of the dielectric functions of the layers, respectively, and employed as a complementary technique to Raman spectroscopy [2–5]. It was shown that infrared spectra of the structures can be described in the framework of the dielectric continuum theory.

Recently, developments of molecular beam epitaxy (MBE) have allowed the fabrication of periodical structures with arrays of self-organized quantum dots (QDs). MBE of materials having a large lattice

* Corresponding author. Tel.:+7-3832-343-551; fax: +7-3832-332-771.
E-mail address: milekhin@thermo.isp.nsc.ru (A.G. Milekhin).

1386-9477/$ - see front matter © 2003 Elsevier B.V. All rights reserved.
doi:10.1016/j.physe.2003.11.023

mismatch leads under certain conditions (Stranski–Krastanov growth mode) to spontaneous formation of dislocation-free small-size QDs [7]. A variety of materials (Ge/Si, (In,Ga,Al)Sb/GaAs, In(As)Sb/InP, Al(Ga)As/InAs) are used for QDs formation [8–13]. Most of the published data related to phonons in QDs were derived from Raman scattering experiments performed in a backscattering from the (0 0 1) surface of the structures which allow only LO and interface phonons in QDs to be observed. To the best of our knowledge, no data on TO phonons in self-assembled QDs are available to date. Moreover, phonon spectra of self-assembled QDs superlattices have not been investigated by Infrared spectroscopy so far.

In this paper, the first study of InAs/AlAs periodical structures with InAs (AlAs) QDs embedded in an AlAs (InAs) matrix by means of Infrared spectroscopy is presented. The results obtained on the vibrational spectra of these structures are compared with those derived from Raman measurements.

2. Experimental

The nanostructures studied were grown by MBE on (0 0 1)-oriented GaAs substrates utilizing Stranski–Krastanov growth mode using a Riber 32P system. The samples with AlAs QDs consisting of 50 or 100 periods (samples A50 and A100, respectively) of AlAs (2.4 monolayers (ML, 1 ML $\approx$ 0.3 nm)) and InAs (12 nm) layers were fabricated on a 1.5 μm InAs buffer doped with silicon atoms ($N_{Si} = 2 \times 10^{18}$ cm^{-3}) at the substrate temperature of 420°C.

Samples with InAs QDs consist of 5 or 10 stacks of superlattices (samples I50 and I100, respectively) separated by 10 nm GaAs spacer layers. Each superlattice is composed of 10 periods of 2.2 ML InAs separated by 8 nm AlAs. Doped GaAs ($N_{Si} = 2 \times 10^{18}$ cm^{-3}) was used as a substrate. The substrate temperature was 450°C during the growth of InAs QDs and the first of 4 nm thick AlAs spacers. Then the temperature was increased up to 590°C and further 4 nm of AlAs was deposited. After the deposition of the nominal amount of island material, the growth was interrupted for 12 s in the case of AlAs islands, and 50 s for InAs QDs. According to RHEED data the transition from a two-dimensional to a three-dimensional growth mode (beginning of island formation) for all the samples occurs after the deposition of 1.8 ML of the island material.

The Raman spectra were measured in a backscattering geometry at $T = 80$ K using a Dilor XY triple and a T-64000 spectrometer with the 514.5 nm line of an Ar^+ laser for excitation. For the study of TO phonons a microscope was employed to focus the light on the 1μm spot on a cleaved (1 1 0)-oriented sample edge. The scattering geometries employed were $z(y,x)\bar{z}$, $y'(x',x')\bar{y}'$ and $y'(z,x')\bar{y}'$ with x, y, z, x', y' parallel to the [1 0 0], [0 1 0], [0 0 1], [1 $\bar{1}$ 0] and [1 1 0] directions, respectively. The resolution was 2 cm^{-1} over the whole spectral range.

The IR reflection spectra were recorded using FTIR spectrometers Bruker IFS-113v and Spectrum 2000 Perkin-Elmer in the spectral range of the optical lattice vibrations of the InAs and AlAs (200–450 cm^{-1}) at a temperature of $T = 80$ K. Spectra were taken at normal incidence of IR light and at off-normal incidence ($\vartheta \approx 70°$) using p-polarized light in order to analyze both the TO and LO vibrational modes in thin layers [5]. The resolution was 1 cm^{-1} over the whole spectral range. The number of scans was 2000.

3. Results and discussion

The structures under investigation were characterized by a high-resolution transmission electron microscopy (HRTEM). Cross-sectional HRTEM images shown in Fig. 1 reveal pyramidal- and ellipsoidal-like shape of InAs and AlAs QDs, respectively. The average sizes of AlAs QDs derived from HRTEM images are 4–5 nm base length and 2–4 nm height. InAs islands have larger base lengths (about 10 nm) with the height of about 1.5 nm.

Figs. 2 and 3 show experimental IR spectra of the samples A50 and I50, respectively (solid lines) measured at off-normal incidence using p-polarized light. A high reflection background is due to the highly doped GaAs substrate and the InAs layer. The strong minima in the spectra of sample A50 (I50) at 216 cm^{-1}(360 cm^{-1}) and 245 cm^{-1} (405 cm^{-1}) correspond to absorption by TO and LO phonons in InAs (AlAs) layers, respectively. IR spectrum of sample I50 reveals prominent features at 260 and 292 cm^{-1} attributed to the low-frequency plasmon–phonon mode from doped GaAs substrate and

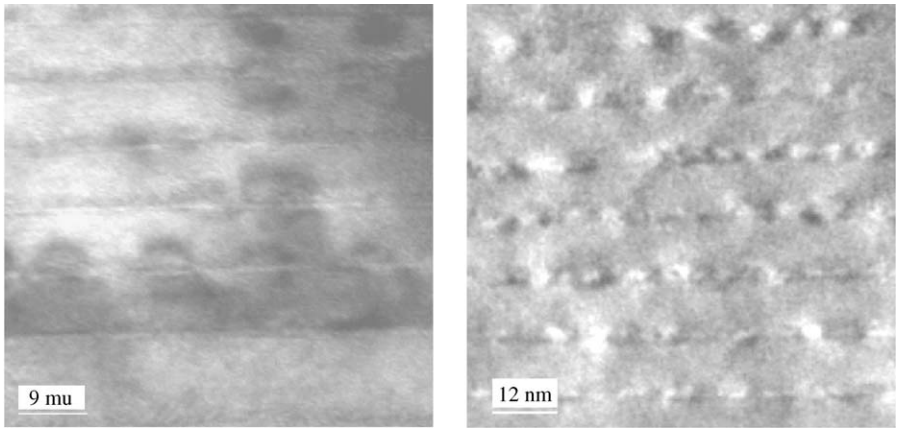

Fig. 1. Cross-sectional HRTEM images of samples (left) I50 and (right) A50.

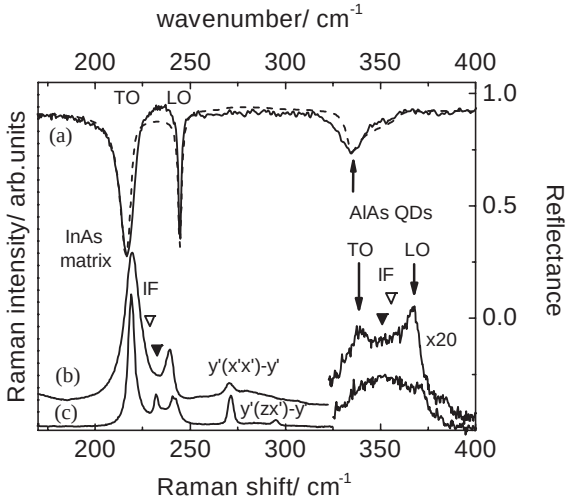

Fig. 2. Infrared reflectivity and Raman spectra of sample A50. IR spectra were measured at off-normal incidence conditions using p-polarised light. Raman spectra were taken in the $y'(x',x')\bar{y'}$ and $y'(z,x')\bar{y'}$ scattering geometries. Calculated IR reflection spectrum is shown by dashed line. The frequency positions of optical phonons localized in QDs and layers are shown by vertical arrows. Solid and open triangles show the frequency position of interface phonons calculated for spheroidal and spherical QDs, respectively.

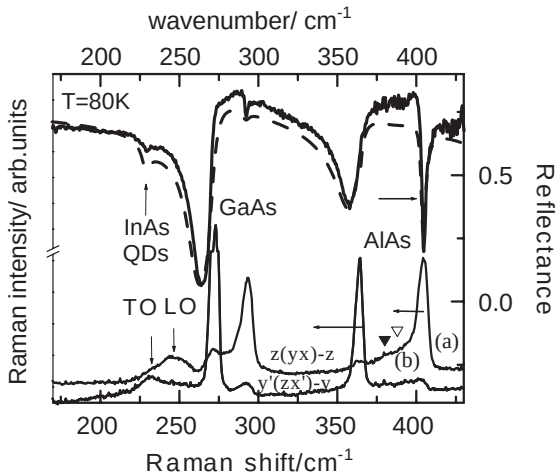

Fig. 3. Infrared reflectivity and Raman spectra of sample I50. IR spectra were measured at off-normal incidence conditions using p-polarised light. Raman spectra were taken in the $y'(x',x')\bar{y'}$ and $z(y,x)\bar{z}$ scattering geometries. Calculated IR reflection spectrum is shown by dashed line. The frequency positions of optical phonons localized in QDs are shown by vertical arrows. Solid and open triangles show the frequency position of interface phonons calculated for spheroidal and spherical QDs, respectively.

LO phonon from GaAs spacer layers. Additional lines in the spectra of sample A50(I50) at about 335 cm^{-1}(229 cm^{-1}) are caused by interaction of IR radiation with AlAs (InAs) QDs. It is worth mentioning that no features were observed in the IR spectra at the frequency positions of LO phonons in the QDs which are expected for planar layered structures with layer thickness of a few monolayers [5]. It means that the dielectric function formalism valid for planar superlattices cannot be anymore applied for the

description of the structures with QDs. The dipole–dipole interaction between the dots can be responsible for the observed bulk-like IR absorption spectrum of QD ensembles which reveal only TO phonon peak [14].

In order to describe the experimental IR spectra, the Raman spectra of sample A50(I50) shown in Fig. 2 (Fig. 3) were measured in different scattering geometries to directly determine TO and LO resonance frequencies of the QDs. The Raman spectra of sample A50 (I50) show strong peaks at 219 and 240 cm^{-1} (364 and 405 cm^{-1}) attributed to TO and LO phonons from InAs (AlAs) layers. Raman lines at 270 and 294 cm^{-1} seen in both figures are due to TO and LO phonons from GaAs. Remarkable features at 339 and 367 cm^{-1} (sample A50) and at 230 and 246 cm^{-1} (sample I50) are attributed to TO and LO phonons localized in AlAs and InAs QDs, respectively, shifted from their bulk position due to tensile and compressive strain in AlAs and InAs QDs, respectively [10]. Confinement in QDs can also affect the Raman spectrum leading to a shift of fundamental optical phonon modes localized in the QDs and the appearance of high-order confined modes. In our structures, such a shift does not exceed 2 cm^{-1} and a distribution of QDs in size smears out the features. As a result only the Raman peaks at frequencies close to the fundamental optical phonon modes can be observed in the spectra. Therefore, confinement effect is negligible in further consideration.

Raman spectra in Fig. 2 reveal, in addition, features located between the frequency position of TO and LO phonons of AlAs QDs and InAs layers (232 and 351 cm^{-1}). These modes are attributed to interface InAs- and AlAs-like modes localized near AlAs/InAs interfaces. Their frequency positions were calculated in the frame of the dielectric continuum model [15]. In the calculation we supposed that AlAs QDs surrounded by InAs have a shape of an ellipsoid with a ratio of the ellipsoid axes 2:1 corresponding to the value derived from HRTEM images. The results of calculation are in good agreement with the experimental data. The frequency positions of InAs- and AlAs-like interface phonons (231 and 350.7 cm^{-1}, respectively) are depicted in the figure by solid triangles. For comparison the frequency positions of interface phonons in the structure with spherical QDs are shown by open triangles.

The determined frequency positions of the optical phonons were further used for fitting of the calculated IR reflection spectra to experimental ones. The shift of 4 cm^{-1} due to different sample temperatures in IR and Raman experiments was taken into account.

In order to describe the IR spectra of the structures with QDs the following model was used. Each matrix layer, a GaAs substrate, an InAs buffer layer are supposed to be isotropic and can be described by the dielectric function

$$\varepsilon(\omega) = \varepsilon_\infty \left(1 + \frac{\omega_{LO}^2 - \omega_{TO}^2}{\omega_{TO}^2 - \omega^2 + i\gamma\omega} - \frac{\omega_p^2}{\omega^2 + i\omega\gamma_p}\right), \quad (1)$$

where ε_∞ is the high-frequency dielectric function and ω_{TO}, ω_{LO}, ω_p, γ, γ_p are, respectively, the frequencies of TO, LO phonons and plasmon frequencies and the damping constant of the phonons and plasmon. The layer with QDs was considered as an effective layer of spherical QDs distributed in a matrix material. The dielectric function of the layer can be written in the effective-medium approximation [16] as

$$(1-f)\frac{\varepsilon_m - \varepsilon_{eff}}{\varepsilon_m + 2\varepsilon_{eff}} + f\frac{\varepsilon^{QD} - \varepsilon_{eff}}{\varepsilon^{QD} + 2\varepsilon_{eff}} = 0, \quad (2)$$

where ε_m, ε^{QD} and f are the dielectric functions of a matrix and a QDs material given by Eq. (1) and the volume fraction of QDs, respectively. The thickness of this layer was taken to be equal to the average height of QDs determined by HRTEM. The volume fraction of QDs is specified by a nominal thickness of a QDs layer during MBE growth. The IR reflection spectra for the multi-layered structures calculated by the method described in [5] are shown in the figures by dashed lines. One can see a good correspondence of the experimental and calculated IR reflection spectra.

Figs. 4 and 5 show experimental and calculated IR reflection spectra of the samples A100 and I100 taken at normal and off-normal incidence conditions. A reflection edge above 400 cm^{-1} is due to the lower concentration of free carries in the doped GaAs substrate and InAs layer. Features observed near 300cm^{-1} in both figures are interference fringes due to IR light interference on the whole thickness of multi-layered structures. One can see that the optical phonons localized in InAs and AlAs QDs are observed at the same

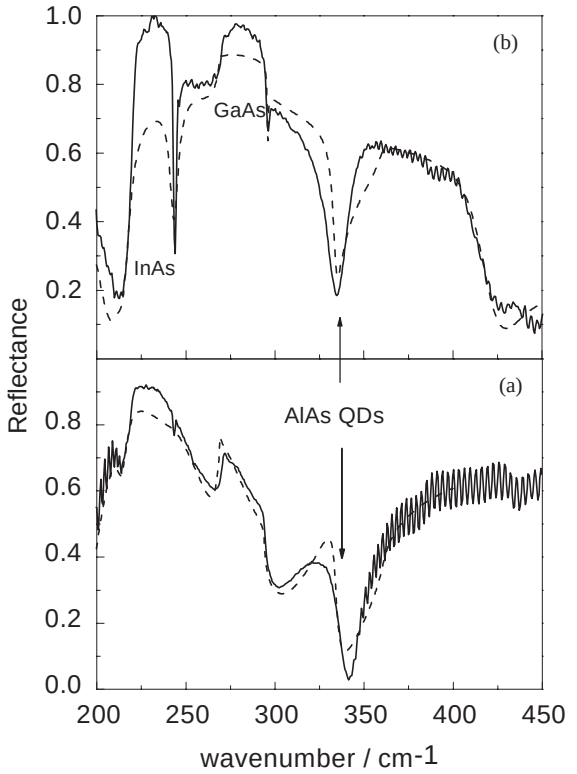

Fig. 4. Experimental IR reflection spectra of sample A100 measured (a) at normal incidence and (b) at off-normal incidence conditions using p-polarised light. Calculated IR reflection spectrum is shown by dashed line. The frequency positions of optical phonons localized in AlAs QDs are shown by vertical arrows.

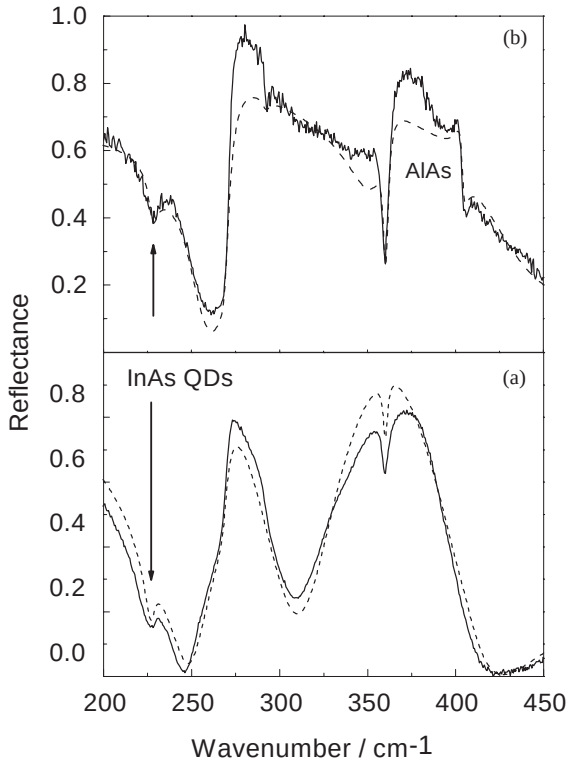

Fig. 5. Experimental IR reflection spectra of sample I100 measured (a) at normal incidence and (b) at off-normal incidence conditions using p-polarised light. Calculated IR reflection spectrum is shown by dashed line. The frequency positions of optical phonons localized in InAs QDs and layers are shown by vertical arrows.

frequency positions as for samples A50 and I50. This confirms the same QDs strain state for the structures with different number of QDs layers. IR spectra were calculated using the model described above. The only fitting parameters which is changed for samples with different number of periods are the plasma frequency and damping coefficients in doped GaAs substrate and InAs layers. A good correspondence of the experimental and calculated IR spectra proves the validity of the approach used.

4. Conclusion

We performed an experimental study of vibrational spectrum of multi-layered InAs/AlAs structures with ensembles of InAs and AlAs QDs using a combination of Raman and IR spectroscopy. LO and TO phonons confined in the QDs and interface phonons were observed in Raman spectra, while IR spectra reveal features at the frequency positions of TO phonons. The positions of experimentally observed interface phonons in QDs and matrix layer agree well with those calculated within the dielectric continuum model. It is shown that the effective medium approximation adequately describes IR reflection spectra of the structures.

Acknowledgements

This work was supported in part by the Volkswagen Foundation (Project I/76837), INTAS (grant YS-2001/2-12/1B/D), FAPESP and the Russian

Foundation for Basic Research (Grant No. 01-02-16969). We are thankful to Mrs. Gisela Baumann for sample preparation for the HRTEM experiments.

References

[1] M. Cardona, G. Guntherodt (Eds.), Light Scattering in Solids, Springer, Berlin, 1989.
[2] Yu. Pusep, et al., JETP Lett. 52 (1990) 464.
[3] G. Scamarcio, et al., Phys. Rev. B 43 (1991) 14754.
[4] Yu. A. Pusep, et al., Phys. Rev. B 52 (1995) 2610.
[5] A.G. Milekhin, et al., JETP Lett. 64 (1996) 393.
[6] P.Y. Yu, M. Cardona, Fundamentals of Semiconductors, Springer, Berlin, Heidelberg, New York, 1999.
[7] D. Bimberg, M. Grundmann, N.N. Ledentsov, Quantum Dot Heterostructures, Wiley, New York, 1999.
[8] J. Groenen, et al., Appl. Phys. Lett. 71 (1997) 3856.
[9] B.R. Bennett, et al., Appl. Phys. Lett. 68 (1996) 958.
[10] D.A. Tenne, et al., Phys. Rev. B 61 (2000) 13785.
[11] Yu. A. Pusep, et al., Phys. Rev. B 58 (1998) R1770.
[12] G. Armelles, et al., J. Appl. Phys. 81 (1997) 6339.
[13] J. Groenen, et al., Appl. Phys. Lett. 69 (1996) 943.
[14] M.I. Vasilevskiy, Phys. Rev. B 66 (2002) 195326.
[15] P.A. Knipp, T.L. Reinecke, Phys. Rev. B 46 (1992) 10310.
[16] D.A.G. Bruggeman, Ann. Phys. 24 (1935) 636.